PRAMANA — journal of physics

Vol. 78, No. 3
March 2012
pp. 451–458

Effective atomic number, electron density and kerma of gamma radiation for oxides of lanthanides

R S NIRANJAN[1,2], B RUDRASWAMY[1] and N DHANANJAYA[1,3,*]
[1]Department of Physics, Bangalore University, Bangalore 560 056, India
[2]Department of Physics, Dravidian University, Kuppam 517 425, India
[3]Department of Physics, B.M.S. Institute of Technology, Bangalore 560 064, India
*Corresponding author. E-mail: dhanu.siri@yahoo.co.in

MS received 26 April 2011; revised 26 September 2011; accepted 21 October 2011

Abstract. An attempt has been made to estimate the effective atomic number, electron density (0.001 to 10^5 MeV) and kerma (0.001 to 20 MeV) of gamma radiation for a wide range of oxides of lanthanides using mass attenuation coefficient from WinXCom and mass energy absorption coefficient from Hubbell and Seltzer. The values of these parameters have been found to change with energy for different oxides of lanthanides. The lanthanide oxides find remarkable applications in the field of medicine, biology, nuclear engineering and space technology. Nano-oxides of lanthanide find applications in display and lighting industry.

Keywords. Effective atomic number; electron density; kerma; oxides of lanthanides.

PACS No. 61.80.−x

1. Introduction

Oxides of lanthanides have many applications in scientific, technological, medical and commercial fields. Cerium oxide is widely used in automobile exhaust catalysts as oxygen storage material. Due to its ability to take and release oxygen under oxidizing and reducing conditions, it replaces silicon dioxide in electronic appliances. Dysprosium oxide is used in cermets as nuclear reaction control rods. Erbium oxide is used as gate dielectric in CMOS logic circuits. Europium oxide is used as an activating ion for colour television phosphors, as control rods in the liquid metal fast breeder reactors and in vacuum deposition. Gadolinium oxide is used in making metal oxide semiconductor field effect transistors. Holmium oxide is used in producing metal halide lamps and also as an additive of various garnets. Lanthanum oxide is used as an ingredient in non-silica, rare element optical glass with oxides of tungsten, tantalum and thorium. Also it is used in X-ray image intensifying screens. Neodymium oxide is used in ceramic capacitors, colour TV tubes, high-temperature glazes, colouring glasses, carbon-arc-light electrodes

DOI: 10.1007/s12043-011-0247-4; ***e*Publication: 28 February 2012**

and vacuum deposition. Samarium oxide is used in optical and infrared absorbing glass to absorb infrared radiation. It is also used as a neutron absorber in control rods for nuclear power reactors. Ytterbium oxide is used in the manufacture of permanent magnet materials, glass, ceramic colouring agents and laser materials. Thulium oxide targets prepared by the polymer-assisted deposition method are used to test the method's feasibility for nuclear science applications by irradiating heavy-ion beams. Oxides of lanthanides are considered as better shielding materials to the exposure of gamma radiation. In this connection, the parameters such as effective atomic number, electron density and kerma turn out to be useful parameters.

Berger *et al* [1] developed XCOM for estimating mass attenuation coefficient and photon interaction cross-section of any element, compound and mixture in the energy range from 1 keV to 100 GeV. XCOM was transformed to the Windows platform by Gerward *et al* [2] and this Windows version is called WinXCom. Manohara *et al* [3] have estimated the effective atomic number and electron density of amino acid in the energy range 1 keV–100 GeV using WinXCom program. Koutroubas [4] proposed a new thin, low-cost, gamma radiation shielding material which is an industrial by-product based on the study of high effective atomic number. Murty [5] reported the effective atomic number in the energy region of absorption edge for W/Cu alloy. Duvauchelle *et al* [6] have developed a new method for estimating effective atomic number for mixtures, compounds and aqueous solutions using Rayleigh to Compton scattering ratio. Nayak *et al* [7] have reported accurate values of effective atomic number for polymers, alloys, compounds and elements at an energy of 59.54 keV. El-Kateb *et al* [8] have estimated the total interaction cross-section and effective atomic number for alloys such as brass (Cu/Zn). Gowda *et al* [9] studied the effective atomic numbers and electron densities of amino acids and sugars in the energy range 30–1333 keV. Shivaramu [10] estimated the effective atomic numbers for photon energy absorption and photon attenuation of tissues from human organs. Bastug *et al* [11] measured the effective atomic number for (PbO, $Na_2B_4O_7 \cdot 10H_2O$) and ($UO_2(NO_3)_2$ mixtures against changing contents of PbO, $Na_2B_4O_7 \cdot 10H_2O$ and $UO_2(NO_3)_2$ in the X-ray energy range from 25 to 58 keV. Singh *et al* [12] have evaluated effective atomic numbers and effective electron densities for some oxides of lanthanides, and alloys of lead and tin of known composition by scattering of 145 keV γ-rays. Han *et al* [13] studied effective atomic numbers and electron densities from mass attenuation coefficients of Ti_xCo_{1-x} and Co_xCu_{1-x} alloys. Kurudirek *et al* [14] studied effective atomic numbers of various alloys for total photon interaction in the energy region of 1 keV–100 GeV. Recently, several investigators have made extensive effective atomic number and electron density studies in a variety of composite materials such as biologically important materials, semiconductors, alloys, dosimetric compounds and glasses. The electronic configuration of lanthanides is not known with certainty. The usual configuration is $4f^n5d^16s^2$ or $4f^{n+1}6s^2$. $5d$ and $4f$ orbitals are so close in energy that it is not always possible to decide whether an electron enters $4f$ or $5d$ orbital. The common oxidation state of lanthanides is $+3$. Lanthanum shows $+3$ oxidation states due to the loss of $6s$ and $5d$ electrons. La^{3+} ion has xenon configuration which is more stable. Similarly, gadolinium and lutetium exhibit only $+3$ oxidation state because removal of three electrons gives the stable $[Xe]4f^7$ configuration for Gd^{3+} ion and $[Xe]4f^{14}$ configuration for Lu^{3+} ion which are in half filled and completely filled conditions. For these, other oxidation states are not possible. Other lanthanides show $+2$ and $+4$ oxidation

Table 1. Various standard values of elements and oxides of lanthanides.

Sample No.	Elements with atomic number	Valence-shell configurations	Oxidation states	Oxides of lanthanides	Molecular formula	Mean atomic number
1	Ce_{58}	$4f^2 5d^0\ 6s^2$	+3,+4	Cerium oxide	Ce_2O_3	28
2	Dy_{66}	$4f^{10} 5d^0\ 6s^2$	+3,+4	Dysprosium oxide	Dy_2O_3	31.2
3	Er_{68}	$4f^{12} 5d^0\ 6s^2$	+3	Erbium oxide	Er_2O_3	32
4	Eu_{63}	$4f^7 5d^0\ 6s^2$	+2,+3	Europium oxide	Eu_2O_3	30
5	Gd_{64}	$4f^7 5d^1\ 6s^2$	+3	Gadolinium oxide	Gd_2O_3	30.4
6	Ho_{67}	$4f^{11} 5d^0\ 6s^2$	+3	Holmium oxide	Ho_2O_3	31.6
7	La_{57}	$4f^0 5d^1\ 6s^2$	+3	Lanthanum oxide	La_2O_3	27.6
8	Lu_{71}	$4f^{14} 5d^0\ 6s^2$	+3	Lutetium oxide	Lu_2O_3	33.2
9	Nd_{60}	$4f^4 5d^0\ 6s^2$	+2,+3,+4	Neodymium oxide	Nd_2O_3	28.8
10	Pr_{59}	$4f^3 5d^0\ 6s^2$	+3,+4	Praseodymium oxide	Pr_2O_3	28.4
11	Sm_{62}	$4f^6 5d^0 6s^2$	+2,+3	Samarium oxide	Sm_2O_3	29.6
12	Tb_{65}	$4f^9 5d^0\ 6s^2$	+3,+4	Terbium oxide	Tb_2O_3	30.8
13	Tm_{69}	$4f^{13} 5d^0\ 6s^2$	+2,+3	Thullium oxide	Tm_2O_3	32.4
14	Yb_{70}	$4f^{14}\ 5d^0\ 6s^2$	+2,+3	Ytterbium oxide	Yb_2O_3	32.8

states. But these states are less stable than +3 oxidation state. Different oxidation states exhibited by lanthanides are indicated in table 1. In literature, there are very few reports on the study of effective atomic number and electron density for oxides of lanthanides. This prompted us to carry out this work. In the present work, the effective atomic numbers and electron densities have been computed for 14 oxides of lanthanides which are shown in table 1 in the energy region of 0.001 MeV to 10^5 MeV using mass attenuation coefficient values from WinXCom. The kerma relative to air has also been computed and reported in the present work. All the estimated values are in good agreement with the reported experimental data [12].

2. Estimation of parameters

2.1 *Effective atomic number and electron density*

The measured intensity I of the transmitted X-ray or γ-ray through a layer of material of thickness x is related to the incident intensity I_0 according to the inverse exponential power law that is usually referred to as Beer–Lambert law.

$$I = I_0 e^{-\mu x} = I_0 e^{-(\mu/\rho)x}, \tag{1}$$

where μ is the mass per unit area (g/cm^2) and (μ/ρ) is the photon mass attenuation coefficient (cm^2/g). For a chemical compound or mixture, the total photon mass attenuation

coefficient $(\mu/\rho)_{\text{comp}}$ has been estimated by the following 'mixture rule' with WinXCom program [2].

$$\left(\frac{\mu}{\rho}\right)_{\text{comp}} = \sum_i \omega_i \left(\frac{\mu}{\rho}\right)_i, \tag{2}$$

where $(\mu/\rho)_i$ and ω_i are respectively the photon mass attenuation coefficient and weight fraction of the ith constituent element present in the given compound. The total cross-section (σ) and different partial cross-sections are related by the relation

$$\sigma = \sigma_{\text{coh}} + \sigma_{\text{incoh}} + \tau + \kappa + \sigma_{\text{ph,n,}}, \tag{3}$$

where σ_{coh} and σ_{incoh} are coherent and incoherent scattering cross-sections, respectively. τ is the atomic photoelectric cross-section, κ is the positron electron pair production cross-section and $\sigma_{\text{ph,n}}$ is the photonuclear cross-section. The effective molecular cross-section (σ_{m}) is estimated using the values of mass attenuation coefficients $(\mu/\rho)_{\text{comp}}$ by the following relation:

$$\sigma_{\text{m}} = \left(\frac{\mu}{\rho}\right)_{\text{comp}} \frac{\sum_i n_i A_i}{N}, \tag{4}$$

where N is the Avogadro's number, n_i and A_i are the total number of atoms and atomic weight of the ith element in a molecule respectively. The effective atomic cross-section (σ_{a}) and effective molecular cross-section (σ_{m}) are related by the following equation:

$$\sigma_{\text{a}} = \frac{\sigma_{\text{m}}}{\sum_i n_i}. \tag{5}$$

Similarly, electronic cross-section (σ_{e}) is given by the following equation:

$$\sigma_{\text{e}} = \frac{1}{N} \sum_i \left(\frac{f_i A_i}{Z_i}\right) \left(\frac{\mu}{\rho}\right)_i, \tag{6}$$

where A_i and $f_i = n_i / \sum_i n_i$ are the atomic number and fractional abundance of the constituent element.

Effective atomic number (Z_{eff}) is the ratio of the atomic and electronic cross-sections.

$$Z_{\text{eff}} = \frac{\sigma_{\text{a}}}{\sigma_{\text{e}}}. \tag{7}$$

The electron density (N_{el}) is the number of electrons per unit mass and is closely related to the effective atomic number. The electron density for a compound is given by

$$N_{\text{el}} = \frac{(\mu/\rho)_{\text{comp}} Z_{\text{eff}}}{\sigma_{\text{a}}}. \tag{8}$$

2.2 *Kerma*

Kerma (K_{a}) has been estimated using the known mass energy absorption coefficient of the compound $(\mu_{\text{en}}/\rho)_{\text{comp}}$ and mass energy absorption coefficient values of air $(\mu_{\text{en}}/\rho)_{\text{air}}$ with the following expression:

$$K_{\text{a}} = \frac{(\mu_{\text{en}}/\rho)_{\text{comp}}}{(\mu_{\text{en}}/\rho)_{\text{air}}}. \tag{9}$$

(μ_{en}/ρ) of both compound and air are estimated using the following relation:

$$(\mu_{en}/\rho) = \sum_i \omega_i \, (\mu_{en}/\rho)_i \, . \tag{10}$$

The values of mass energy absorption coefficient of the ith element, $(\mu_{en}/\rho)_i$, at various energies are taken from Hubbell and Seltzer [15].

3. Results and discussion

The variations of Z_{eff} and N_{el} are shown in figures 1 and 2. It can be seen that the variations of Z_{eff} and N_{el} with energy are approximately similar for all the oxides of lanthanides studied. The values of Z_{eff} and N_{el} steadily increase up to 0.01 MeV, remain constant up to 0.1 MeV, then they steadily decrease up to 1 MeV, then increase sharply up to 100 MeV, after which they almost remain constant up to 10^5 MeV. The Z_{eff} and N_{el} values show a broad peak and a maximum value at 0.01 MeV and minima at 1 MeV for all oxides of lanthanides. The variation of Z_{eff} with energy may be attributed to the relative domination of the partial processes, viz. photoelectric effect, coherent scattering, incoherent scattering and pair production [10]. At low energies the photoelectric effect is dominant and hence Z_{eff} for the photon absorption is mainly described by Z_{eff} for this partial process. Similarly, at higher energies the contribution due to scattering and pair production process will be more in comparison with photoelectric effect and this will have its effect on Z_{eff} for photon absorption. Hence at low energies, where photoelectric effect dominates, Z_{eff}

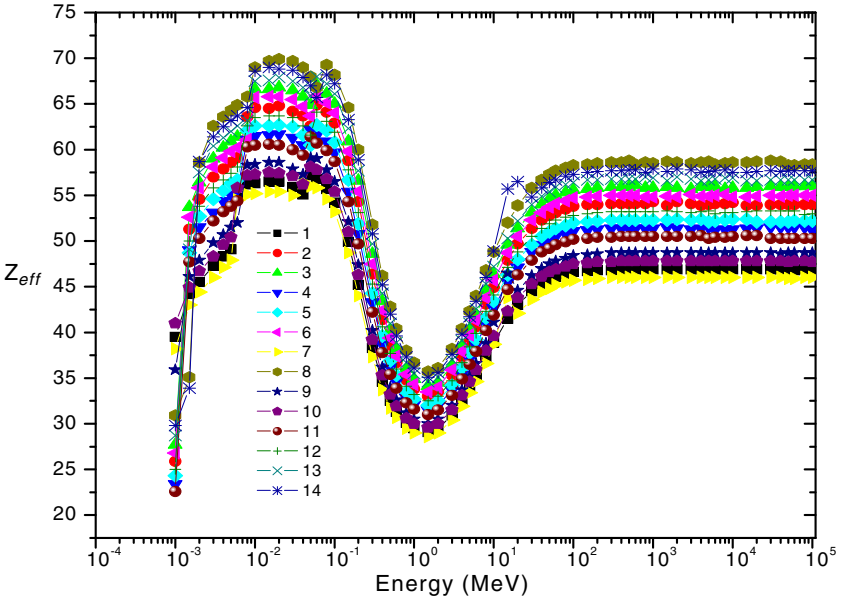

Figure 1. Energy dependence of Z_{eff} for total photon interaction with coherent scattering (labels 1–14 refer to the compounds shown in table 1, in the same order).

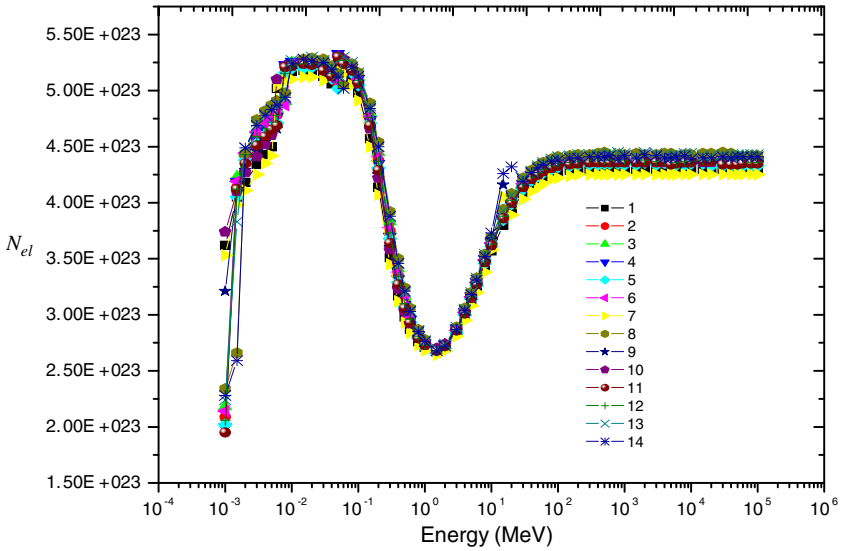

Figure 2. Energy dependence of N_{el} for total photon interaction (with coherent scattering).

value is more and at higher energies, where the scattering and pair production process dominate, the Z_{eff} value is less. Therefore, Z_{eff} for photon energy absorption varies from a higher value at lower energies to a lower value at higher energies with a peak due to photoelectric effect around the K-absorption edge of the high-Z constituent of the compound studied, depending on the relative domination of one γ-ray process over the other. Almost similar behaviour is seen in the variation of N_{el} as a function of energy. Table 2 shows the present values of Z_{eff} compared to the experimental results at 145 keV of previous workers [12] which shows a good agreement between them.

The K_{a} values estimated using expression (9) are plotted as a function of energy in figure 3. The K_{a} values show a peak due to the photoelectric effect around the K-absorption edge of the high-Z constituent of the compound. The K_{a} values also show a broad peak around 0.06 MeV for all oxides of lanthanides. From figure 3 it may be seen that the variation of K_{a} with energy below the K-absorption edge of high-Z element present in the

Table 2. Theoretical and experimental values of Z_{eff}, for 145 keV photon energy.

Oxides of lanthanides	Experimental values [12]	Theoretical values [12]	Present work (theoretical values)
La_2O_3	52.2 ± 1.2	53.4	49.2
Pr_2O_3	54.8 ± 1.0	55.4	51.5
Eu_2O_3	57.5 ± 1.1	59.4	56.0
Gd_2O_3	60.8 ± 1.0	60.4	57.1
Tb_2O_3	62.2 ± 0.9	61.3	58.2
Dy_2O_3	63.9 ± 0.9	62.3	59.3

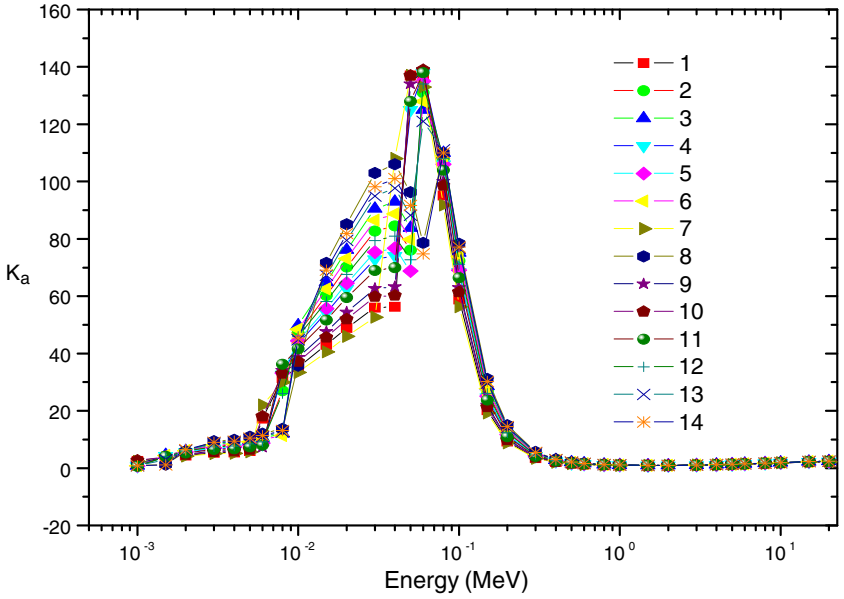

Figure 3. Energy dependence of the kerma.

compound, is not uniform because of the nonuniform variation of (μ_{en}/ρ) at a particular energy.

4. Conclusions

We reported new data on Z_{eff} and N_{el} in the energy region of 0.001 to 10^5 MeV and on K_a in the energy region 0.001 to 20 MeV for selected pure oxides of lanthanides. It is expected that these new data are useful in the field of radiation shielding. Also, to the best of the knowledge of the authors, these data are the first of these kind estimated for a wide energy range.

Acknowledgements

The authors are grateful to Prof. L Gerward, Department of Physics, Technical University of Denmark, for providing the computer program WinXCom.

References

[1] M J Berger and J H Hubbell, XCOM: Photon Cross Sections Database, Web Version 1.2, available at http://physics.nist.gov/xcom (1987/99)
[2] L Gerward, N Guilbert, K B Jensen and H Levring, *Rad. Phys. Chem.* **71**, 653 (2004)

[3] S R Manohara and S M Hanagodimath, *Nucl. Instrum. Methods Phys. Res.* **B264**, 9 (2007)
[4] S K Koutroubas, *J. Radiol. Prot.* **12**, 37 (1992)
[5] V R K Murty, *Rad. Phys. Chem.* **71**, 667 (2004)
[6] P Duvauchelle, G Peix and D Babot, *Nucl. Instrum. Methods* **B155**, 221 (1999)
[7] N G Nayak, M G Vijaya and K Siddappa, *Radiat. Phys. Chem.* **61**, 559 (2001)
[8] A H El-Kateb, R A M Rizk and A M Abdul-Kader, *Ann. Nucl. Energy* **27**, 1333 (2000)
[9] S Gowda, S Krishnaveni and R Gowda, *Nucl. Instrum. Methods* **B239**, 361 (2005)
[10] Shivaramu, *Medical dosimetry* **27(1)**, 1 (2002)
[11] A Bastug, A Gurol, O Icelli and Y Sahin, *Ann. Nucl. Energy* **37**, 927 (2010)
[12] M P Singh, Amandeep Sharma, Bhajan Singh and B S Sandhu, *Radiation measurements*, DOI: 10.1016/j.radmeas.2010.01.021 (2010)
[13] L Han and L Demir, *Nucl. Instrum. Methods* **B267**, 3505 (2009)
[14] M Kurudirek, M Buyukydz and Y Ozdemir, *Nucl. Instrum. Methods* **A613**, 251 (2010)
[15] J H Hubbell and S M Seltzer, Report, NISTIR-5632 (1995)